

Variational calculation of ${}^4\text{He}$ tetramer ground and excited states using a realistic pair potential

E. Hiyama*

RIKEN Nishina Center, RIKEN, Wako 351-0198, Japan

M. Kamimura†

Department of Physics, Kyushu University, Fukuoka 812-8581, Japan,
RIKEN Nishina Center, RIKEN, Wako 351-0198, Japan

(Dated: October 8, 2018)

We calculated the ${}^4\text{He}$ trimer and tetramer ground and excited states with the LM2M2 potential using our Gaussian expansion method (GEM) for *ab initio* variational calculations of few-body systems. The method has extensively been used for a variety of three-, four- and five-body systems in nuclear physics and exotic atomic/molecular physics. The trimer (tetramer) wave function is expanded in terms of symmetric three-(four-)body Gaussian basis functions, ranging from very compact to very diffuse, without assuming any pair correlation function. Calculated results of the trimer ground and excited states are in excellent agreement with the literature. Binding energies of the tetramer ground and excited states are obtained to be 558.98 mK and 127.33 mK (0.93 mK below the trimer ground state), respectively. We found that precisely the same shape of the short-range correlation ($r_{ij} \lesssim 4\text{\AA}$) in the dimer appear in the ground and excited states of trimer and tetramer. The overlap function between the trimer excited state and the dimer and that between the tetramer excited state and the trimer ground state are almost proportional to the dimer wave function in the asymptotic region (up to $\sim 1000\text{\AA}$). Also the pair correlation functions of trimer and tetramer excited states are almost proportional to the squared dimer wave function. We then come to propose a model which predicts the binding energy of the first excited state of ${}^4\text{He}_N$ ($N \geq 3$) measured from the ${}^4\text{He}_{N-1}$ ground state to be nearly $\frac{N}{2(N-1)}B_2$ using the dimer binding energy B_2 .

I. INTRODUCTION

In early 1970's, Efimov pointed out a possibility of having an infinite number of three-body bound states even when none exists in the separate two-body subsystems [1–3]. This occurs when the two-body scattering length is much larger than the range of the two-body interaction. As a candidate of such three-body states, Efimov discussed about the famous Hoyle state [4] (the second 0^+ state at 7.65MeV in the ${}^{12}\text{C}$ nucleus) taking a model of three α particles (clusters of three ${}^4\text{He}$ nuclei) as well as about the three-nucleon bound state (${}^3\text{H}$ nuclei). In nuclear systems, the Borromean states, weakly bound three-body states though having no bound two-body subsystems, are familiar but not classified as Efimov states.

In atomic systems, triatomic ${}^4\text{He}$ (trimer) have been expected to have bound states of Efimov type since the realistic ${}^4\text{He}$ - ${}^4\text{He}$ interactions [5? –8] give a large ${}^4\text{He}$ - ${}^4\text{He}$ scattering length ($\simeq 115\text{\AA}$), much greater than the potential range ($\sim 10\text{\AA}$), and a very small ${}^4\text{He}$ dimer binding energy ($\simeq 1.3\text{ mK}$). (Experimentally, Ref. [10] evaluated a scattering length of 104_{-18}^{+8}\AA and a binding energy of $1.1_{-0.2}^{+0.3}\text{ mK}$).

As is mentioned in recent reviews about the ${}^4\text{He}$ trimer [11, 12] (further references therein), i) a lot of three-body calculations using the realistic pair poten-

tials have shown that the ${}^4\text{He}$ trimer possesses two bound states with binding energies of nearly 126.4 mK and 2.3 mK, ii) it is already rather well established that, if the ${}^4\text{He}$ trimer excited state exist, it should be Efimov nature, and iii) it is suggested that the ${}^4\text{He}$ trimer ground state may be considered as an Efimov state since the ground- and excited-state binding energies move along the same universal scaling curve under any small deformation of the two-body potential (for details, see, e.g., Sec.III of Ref. [13]). Experimentally, the ${}^4\text{He}$ trimer ground state has been observed in Ref. [14] to have the ${}^4\text{He}$ - ${}^4\text{He}$ bond length of 11_{-5}^{+4}\AA in agreement with theoretical predictions, whereas a reliable experimental evidence for the ${}^4\text{He}$ trimer excited state is still missing.

Only very recently, experimental evidences of Efimov trimer states have been reported in the work using the ultracold gases of cesium atoms [15, 16], potassium atoms [17], lithium-7 atoms [18, 19], and lithium-6 atoms [20–24], in which the two-body interaction between those alkali atoms was manipulated so as to tune the scattering length to values significantly greater than the potential range. These experiments have been accessing the study of a wide variety of interesting physical systems in the atomic and nuclear fields. Recently, the study extends to the Efimov physics and universality of four-atomic systems (tetramers).

Though the interactions between ${}^4\text{He}$ atoms can not be manipulated, the study of ${}^4\text{He}$ trimer using the realistic pair potentials has been providing fundamental information to the Efimov physics. Now it is one of the challenging subjects to precisely investigate the structure

*Electronic address: hiyama@riken.jp

†Electronic address: mkamimura@riken.jp

of ${}^4\text{He}$ tetramer using the realistic ${}^4\text{He}$ - ${}^4\text{He}$ potential.

So far there exist in the literature a large number of ${}^4\text{He}$ trimer calculations [25–39] giving well converged results with the realistic ${}^4\text{He}$ - ${}^4\text{He}$ interactions. However, calculations of the tetramer remain limited [25, 28–31]; in those papers, the binding energy of the tetramer ground state agrees well with each other, while that of the loosely bound excited state differs significantly from one another.

Thus the main purpose of the present paper is to perform accurate calculations of the ${}^4\text{He}$ tetramer ground and excited states using a realistic ${}^4\text{He}$ - ${}^4\text{He}$ interaction, the LM2M2 potential [6]. We employ the Gaussian expansion method (GEM) for *ab initio* variational calculations of few-body systems [40–43]. The method has been proposed and developed by the present authors and collaborators and applied to various types of three-, four- and five-body systems in nuclear physics and exotic atomic/molecular physics (cf. review papers [43–45]).

Advantage of using the GEM for the ${}^4\text{He}$ tetramer calculation in the presence of the strong short-range repulsive potential is as follows: Some 30000 symmetrized four-body Gaussian basis functions, ranging from very compact to very diffuse, are constructed on the full 18 sets of Jacobi coordinates without assuming any pair correlation function. They form a nearly complete set in the finite coordinate space concerned, so that one can describe accurately both the short-range structure and the long-range asymptotic behavior (up to ~ 1000 Å) of the four-body wave function, which makes it possible to find new facets of ${}^4\text{He}$ clusters.

We thus find that precisely the same shape of the short-range correlation ($r_{ij} \lesssim 4$ Å) in dimer appears in the ground and excited states of trimer and tetramer. This gives a foundation to an *a priori* assumption that a two-particle correlation function (such as the Jastrow’s) so as to simulate the short-range part of the dimer wave function is incorporated in the trimer and tetramer wave functions from the beginning.

By illustrating the asymptotic behavior of the ${}^4\text{He}$ trimer and tetramer, we discuss about an interesting relation between their excited-state wave functions and the dimer wave function. We then come to propose a ‘dimerlike-pair’ model that predicts the binding energy of the first excited state of the N -cluster system, ${}^4\text{He}_N$, measured from the ground state of ${}^4\text{He}_{N-1}$ to be approximately $\frac{N}{2(N-1)}B_2$ using the dimer binding energy B_2 .

We explicitly write the asymptotic form of the total wave function of ${}^4\text{He}$ trimer (tetramer). The asymptotic normalization coefficient (ANC) [26, 41, 46–48], namely the amplitude of tail function of the dimer-atom (trimer-atom) relative motion in the present case, is a quantity to reflect the internal structure of trimer (tetramer). Therefore, attention to the ANC might be useful when one intends to reproduce the non-universal variation of the ${}^4\text{He}$ trimer (tetramer) states by means of parametrizing effective models beyond Efimov’s universal theory.

The paper is organized as follows: In Sec. II, we apply the GEM to the three-body calculation of the ${}^4\text{He}$ trimer

ground and excited states showing that the calculated results agree excellently with the literature. In Sec. III, the four-body calculation of the ${}^4\text{He}$ tetramer ground and excited states is presented. Summary is given in Sec. IV.

II. ${}^4\text{He}$ TRIMER

The ${}^4\text{He}$ trimer bound states have extensively been studied in many theoretical work using realistic potentials. Monte-Carlo, hyperspherical, variational and Faddeev techniques were used to calculate accurately the binding energies of the ground and excited states [25–39] (see also recent reviews [11, 12]). Nevertheless, in this section, we explain our Gaussian expansion method (GEM) and present the calculated result for the ${}^4\text{He}$ trimer in order to demonstrate high accuracy of our calculation before we report our investigation of the ${}^4\text{He}$ tetramer in the next section.

A. Three-body wave function

We take all the three sets of Jacobi coordinates (Fig. 1), $\mathbf{x}_1 = \mathbf{r}_2 - \mathbf{r}_3$ and $\mathbf{y}_1 = \mathbf{r}_1 - \frac{1}{2}(\mathbf{r}_2 + \mathbf{r}_3)$ and cyclically for $(\mathbf{x}_2, \mathbf{y}_2)$ and $(\mathbf{x}_3, \mathbf{y}_3)$, \mathbf{r}_i being the position vector of i th particle. Hamiltonian of the system is expressed as

$$H = -\frac{\hbar^2}{2\mu_x}\nabla_x^2 - \frac{\hbar^2}{2\mu_y}\nabla_y^2 + \sum_{1=i<j}^3 V(r_{ij}), \quad (2.1)$$

where $\mu_x = \frac{1}{2}m$ and $\mu_y = \frac{2}{3}m$, m being mass of a ${}^4\text{He}$ atom. $V(r_{ij})$ is the two-body ${}^4\text{He}$ - ${}^4\text{He}$ potential as a function of the pair distance $\mathbf{r}_{ij} = \mathbf{r}_j - \mathbf{r}_i$.

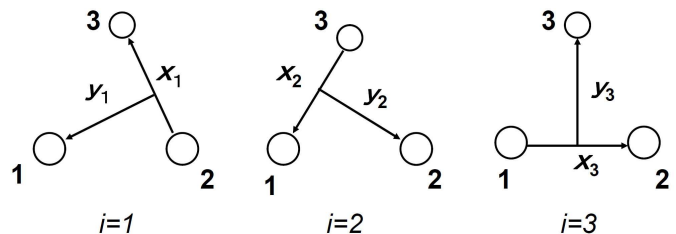


FIG. 1: Three sets of the Jacobi coordinates for ${}^4\text{He}$ trimer.

We calculate the three-body bound-state wave function, Ψ_3 , which satisfies the Schrödinger equation

$$(H - E)\Psi_3 = 0. \quad (2.2)$$

Since we consider the ${}^4\text{He}$ atom as a spinless boson, we expand the wave function of three identical spinless bosons in terms of L^2 -integrable, fully symmetric three-body basis functions:

$$\Psi_3 = \sum_{\alpha=1}^{\alpha_{\max}} A_{\alpha} \Phi_{\alpha}^{(\text{sym})}, \quad (2.3)$$

$$\Phi_{\alpha}^{(\text{sym})} = \Phi_{\alpha}(\mathbf{x}_1, \mathbf{y}_1) + \Phi_{\alpha}(\mathbf{x}_2, \mathbf{y}_2) + \Phi_{\alpha}(\mathbf{x}_3, \mathbf{y}_3). \quad (2.4)$$

It is of importance that those basis functions $\{\Phi_\alpha^{(\text{sym})}; \alpha = 1, \dots, \alpha_{\text{max}}\}$, which are nonorthogonal to each other, are constructed on the full three sets of Jacobi coordinates; this makes the function space of $\{\Phi_\alpha^{(\text{sym})}\}$ quite wide.

The eigenenergies E and amplitudes A_α of the ground and excited states are determined by the Rayleigh-Ritz variational principle:

$$\langle \Phi_\alpha^{(\text{sym})} | H - E | \Psi_3 \rangle = 0, \quad (2.5)$$

where $\alpha = 1, \dots, \alpha_{\text{max}}$. Eqs.(2.5) results in a generalized eigenvalue problem:

$$\sum_{\alpha'=1}^{\alpha_{\text{max}}} [\mathcal{H}_{\alpha,\alpha'} - E \mathcal{N}_{\alpha,\alpha'}] A_{\alpha'} = 0. \quad (2.6)$$

The matrix elements are written as

$$\mathcal{H}_{\alpha,\alpha'} = \langle \Phi_\alpha^{(\text{sym})} | H | \Phi_{\alpha'}^{(\text{sym})} \rangle, \quad (2.7)$$

$$\mathcal{N}_{\alpha,\alpha'} = \langle \Phi_\alpha^{(\text{sym})} | 1 | \Phi_{\alpha'}^{(\text{sym})} \rangle. \quad (2.8)$$

The lowest-lying two S -wave eigenstates, $\Psi_3^{(v)}$ ($v = 0, 1$), will be identified as the trimer ground ($v = 0$) and excited ($v = 1$) states.

We express each basis function $\Phi_\alpha(\mathbf{x}_i, \mathbf{y}_i)$ as a product of a function of \mathbf{x}_i and that of \mathbf{y}_i :

$$\Phi_\alpha(\mathbf{x}_i, \mathbf{y}_i) = \phi_{n_x l_x}(x_i) \psi_{n_y l_y}(y_i) \left[Y_{l_x}(\hat{\mathbf{x}}_i) Y_{l_y}(\hat{\mathbf{y}}_i) \right]_{JM}, \quad (2.9)$$

where α specifies a set of quantum numbers

$$\alpha = \{n_x l_x, n_y l_y, JM\}$$

commonly for the components $i = 1, 2, 3$. J is the total angular momentum and M is its z -component. In this paper, we consider the trimer bound states with $J = 0$. Then, the totally symmetric three-body wave function requires $l_x = l_y = \text{even}$.

One of the most important issues of the present variational calculation is what type of radial shape we use for $\phi_{n_x l_x}(x_i)$ and $\psi_{n_y l_y}(y_i)$. The basis functions should be capable of precisely describing the strong short-range correlation (without assuming any correlation function *a priori*) and the long-range asymptotic behavior of very loosely bound states.

The GEM recommends two types of functions which are tractable in few-body calculations and work accurately. One is the Gaussian function and the other, more powerful one, is the complex-range Gaussian function [43]. In the next subsection, we introduce the former that was successfully used in our previous study (Sec. 3.1 of Ref. [43]) of the ^4He trimer ground and excited state with the use of the HFDHE2 potential [5]. The latter function is introduced in Sec.II.C.

B. Gaussian basis functions

The radial function $\phi_{n_x l_x}(x)$ in (2.9) is taken to be a Gaussian multiplied by x^{l_x} (similarly for $\psi_{n_y l_y}(y)$):

$$\phi_{n_x l_x}(x) = x^{l_x} e^{-(x/x_{n_x})^2}, \quad (2.10)$$

$$\psi_{n_y l_y}(y) = y^{l_y} e^{-(y/y_{n_y})^2}, \quad (2.11)$$

where normalization constants are omitted for simplicity.

Setting of the ranges by stochastic or random choice does not seem suitable for describing the strong short-range correlation and the long-range asymptotic behavior of the wave function. Any intended choice of the ranges is necessary. The GEM recommends to set them in a *geometric* progression:

$$x_{n_x} = x_1 a_x^{n_x - 1} \quad (n_x = 1, \dots, n_x^{\text{max}}), \quad (2.12)$$

$$y_{n_y} = y_1 a_y^{n_y - 1} \quad (n_y = 1, \dots, n_y^{\text{max}}), \quad (2.13)$$

with common ratios $a_x > 1$ and $a_y > 1$. This greatly reduces the nonlinear parameters to be optimized. We designate a set of the geometric sequence by $\{n_x^{\text{max}}, x_1, x_{n_x^{\text{max}}}\}$ instead of $\{n_x^{\text{max}}, x_1, a_x\}$ and similarly for $\{n_y^{\text{max}}, y_1, y_{n_y^{\text{max}}}\}$, which is more convenient to consider the spatial distribution of the basis set. Optimization of the nonlinear range parameters is in principle by trial and error procedure but much of experiences and systematics have been accumulated in many studies using the GEM.

The basis functions $\{\phi_{nl}\}$ have the following properties: i) They range from very compact to very diffuse, more densely in the inner region than in the outer one. While the basis functions with small ranges are responsible for describing the short-range structure of the system, the basis with longest-range parameters are for the asymptotic behavior. ii) They, being multiplied by normalization constants for $\langle \phi_{nl} | \phi_{nl} \rangle = 1$, have a relation

$$\langle \phi_{nl} | \phi_{n+kl} \rangle = \left(\frac{2a^k}{1+a^{2k}} \right)^{l+3/2}, \quad (2.14)$$

which tells that the overlap with the k -th neighbor is *independent* of n , decreasing gradually with increasing k .

We then expect that the coupling among the whole basis functions take place smoothly and coherently so as to describe properly both the short-range structure and long-range asymptotic behavior simultaneously. We note that a single Gaussian decays quickly as x increases, but appropriate superposition of many Gaussians can decay even exponentially up to a sufficiently large distance. A good example is shown in Fig. 3 of Ref. [43] for the ^4He dimer wave function (with the HFDHE2 potential) that is accurate up to $\sim 1000 \text{ \AA}$ with the use of the nonlinear parameters $\{n^{\text{max}} = 60, x_1 = 0.14 \text{ \AA}$ and $x_{n^{\text{max}}} = 700 \text{ \AA}\}$ (the same-quality dimer wave function is seen in Fig. 2 below in Sec.II.D using the complex-range Gaussians with the LM2M2 potential).

A lot of successful examples of the three- and four-body GEM calculations are shown in review papers [43–45] and

in papers of five-body calculations [49, 50]. The examples includes our previous calculation of the ground and excited states of ${}^4\text{He}$ trimer using the HFDHE2 potential; the binding energies were in good agreement with those given by a Feddeev-equation calculation [33]. As for the trimer wave function, we showed, in Figs. 3, 13 and 14 in Ref.[43], that the strong short-range correlation ($x \lesssim 4$ Å) and asymptotic behavior (up to $x \sim 1000$ Å) of the trimer ground and excited states are simultaneously well described. Also, the three-body basis functions (2.9)–(2.13) together with the LM2M2 potential were used recently by Naidon, Ueda and one of the present authors (E. H.) [51] to study the universality and the three-body parameter of ${}^4\text{He}$ trimers.

C. Complex-range Gaussian basis functions

Before we proceed to the calculation of the ${}^4\text{He}$ tetramer ground and excited states, we improve the Gaussian shape of the basis functions so as to have more sophisticated (but still tractable) radial dependence. We then test the new basis in the calculation of the trimer states below.

In Ref. [43], we proposed to improve the Gaussian shape by introducing *complex* range instead of the real one:

$$\phi_{nl}^{(\omega)}(x) = x^l e^{-(1+i\omega)(x/x_n)^2}, \quad (2.15)$$

where $n = 1, \dots, n_x^{\max}$ and x_n are given by (2.12). Using $\phi_{nl}^{(\pm\omega)}(x)$, we construct two kinds of *real* basis functions:

$$\begin{aligned} \phi_{nl}^{(\cos)}(x) &= x^l e^{-(x/x_n)^2} \cos \omega(x/x_n)^2 \\ &= [\phi_{nl}^{(-\omega)}(x) + \phi_{nl}^{(\omega)}(x)]/2, \end{aligned} \quad (2.16)$$

$$\begin{aligned} \phi_{nl}^{(\sin)}(x) &= x^l e^{-(x/x_n)^2} \sin \omega(x/x_n)^2 \\ &= [\phi_{nl}^{(-\omega)}(x) - \phi_{nl}^{(\omega)}(x)]/2i, \end{aligned} \quad (2.17)$$

where we usually take $\omega = 1$. The three-body basis function $\Phi_\alpha(\mathbf{x}_i, \mathbf{y}_i)$ in (2.9) is replaced by

$$\Phi_\alpha(\mathbf{x}_i, \mathbf{y}_i) = \phi_{n_x l_x}^{(\cos)}(x) \psi_{n_y l_y}(y_i) \left[Y_{l_x}(\hat{\mathbf{x}}_i) Y_{l_y}(\hat{\mathbf{y}}_i) \right]_{JM}, \quad (2.18)$$

where α specifies a set

$$\alpha \equiv \{ \text{'cos' or 'sin'}, \omega, n_x l_x, n_y l_y, JM \}. \quad (2.19)$$

The new basis $\{\phi_{n_x l_x}^{(\cos)}(x)\}$ apparently extend the function space from the old ones (2.10) since they have the oscillating components; see Sec.2.4 and Sec.2.5 of Ref. [43] for some examples taking this advantage in calculations of highly vibrational excited states (with ~ 25 nodes) and scattering states. The *sin*-type basis (2.17) particularly work when the wave function is extremely suppressed at $x \sim 0$ due to the strongly repulsive short-range potential.

In the following calculations, we employ the new basis (2.16) and (2.17) for the x -space instead of (2.10), but keep (2.11) for the y -space.

Note that, when calculating the matrix elements (2.7) and (2.8) using $\phi_{nl}^{(\cos)}(x)$ and $\phi_{nl}^{(\sin)}(x)$, we explicitly take (2.15) and the right-most expression of (2.16) and (2.17) since the computation programming is almost the same as that for (2.10) though some of real variables are changed to complex ones.

A great advantage of the real- and complex-range Gaussian basis functions is that the calculation of matrix elements (2.7) and (2.8) is easily performed. As for the overlap and kinetic-energy matrix elements of the trimer (tetramer), all the six-(nine-)dimensional integrals give analytical expression. In the case of the potential matrix, we have analytical expression except for the one-dimensional numerical integral having the final form

$$\int_0^\infty x^{2m} e^{-\lambda x^2} V(x) x^2 dx. \quad (2.20)$$

We explained, in Ref. [43], various techniques to perform the three- and four-body matrix-element calculations as easily, accurately and rapidly as possible.

It is to be emphasized that the GEM few-body calculations need neither introduction of any *a priori* pair correlation function (such as the Jastrow function) nor separation of the coordinate space by $x < r_c$ and $x > r_c$, r_c being the radius of a strongly repulsive core potential. Proper short-range correlation and asymptotic behavior of the total wave function are *automatically* obtained by solving the Schrödinger equation (2.2) using the above basis functions for *ab initio* calculations.

D. Pair interaction and ${}^4\text{He}$ dimer

To describe the interaction between the ${}^4\text{He}$ atoms, we employ one of the most widely used ${}^4\text{He}$ - ${}^4\text{He}$ interactions, the LM2M2 potential by Aziz and Slaman [6]. Use is made of $\frac{\hbar^2}{m} = 12.12 \text{ KÅ}^2$ as the input mass of ${}^4\text{He}$ atom. We can then precisely compare calculated results for the tetramer ground and excited states with those obtained by Lazauskas and Carbonell [25] who made a Faddeev-Yakubovsky (FY) equation calculation taking the same potential and ${}^4\text{He}$ mass as above. Recently, the authors of Ref. [52] claim that a more precise value of $\frac{\hbar^2}{m} = 12.11928 \text{ KÅ}^2$ should be employed. We shall additionally show the trimer and tetramer binding energies in the case of using this value.

We calculated the ${}^4\text{He}$ dimer binding energy, say B_2 , and the wave function, $\Psi_2(\equiv \Psi_2(x) Y_{00}(\hat{\mathbf{x}}))$, using the same prescription as described above. We expanded $\Psi_2(x)$ with 100 basis functions of (2.16) and (2.17) as

$$\Psi_2(x) = \sum_{n=1}^{n_x^{\max}} [A_n^{(\cos)} \phi_{n0}^{(\cos)}(x) + A_n^{(\sin)} \phi_{n0}^{(\sin)}(x)] \quad (2.21)$$

with a parameter set

$$\{n_x^{\max} = 50, x_1 = 0.5 \text{ Å}, x_{n_x^{\max}} = 600.0 \text{ Å}, \omega = 1.0\}. \quad (2.22)$$

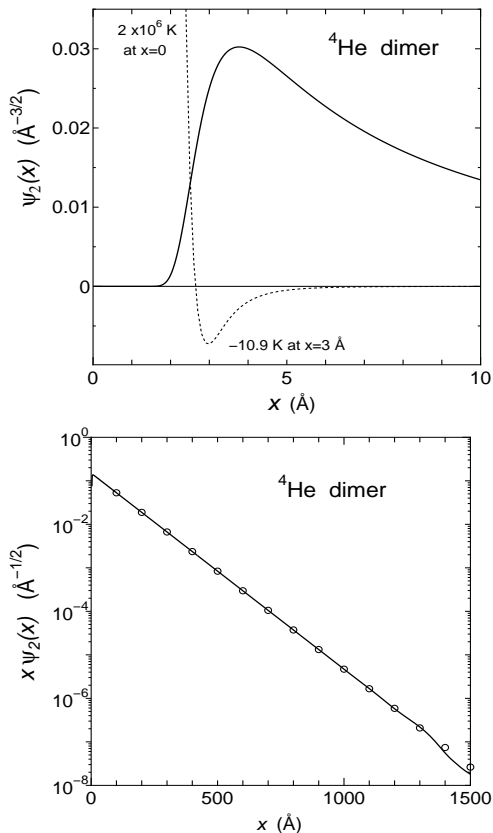


FIG. 2: Short-range structure (upper) and asymptotic behavior (lower) of the radial wave function $\Psi_2(x)$ of the ^4He dimer obtained by using the complex-range Gaussian basis functions (2.21) and (2.22). The open circles stands for the exact asymptotic form. The dotted line (upper) illustrates the LM2M2 potential in arbitrary unit.

We obtained $B_2 = 1.30348$ mK, $\sqrt{\langle x^2 \rangle} = 70.93$ Å, and $\langle x \rangle = 52.00$ Å which are the same as those obtained in the literature. Experimentally, $\langle x \rangle = 52 \pm 4$ Å [10] from which $B_2 = 1.1_{-0.2}^{+0.3}$ mK was estimated.

As shown in Fig. 2, both the strong short-range correlation ($x \lesssim 4$ Å) and the asymptotic behavior of the dimer are well described. In the lower panel, $x\Psi_2(x)$ precisely reproduces the exact asymptotic shape $0.1498 \exp(-\kappa_2 x)$ (Å $^{-1/2}$) with $\kappa_2 = \sqrt{mB_2}/\hbar = 0.0104$ Å $^{-1}$ up to $x \sim 1200$ Å which is large enough for our discussions.

There are 30 basis functions whose Gaussian ranges $x_{n_x} < 4$ Å, which is sufficiently dense to describe the short-range structure of the wave function precisely. An interesting issue is whether the same shape of the short-range correlation in Fig. 2 appear also in the trimer and tetramer ground and excited states without assuming any two-body correlation function.

TABLE I: Mean values for ^4He trimer ground and excited states with the use of the LM2M2 potential and $\frac{\hbar^2}{m} = 12.12$ KÅ 2 . $B_3^{(v)}$ is the binding energy, r_{ij} stands for interparticle distance and r_{iG} is the distance of a particle from the center-of-mass of the trimer. See text for the asymptotic normalization coefficient $C_3^{(v)}$ ($v = 0, 1$).

trimer	ground state			
	present	Ref.[25]	Ref.[26]	Ref.[27]
$B_3^{(0)}$ (mK)	126.40	126.39	126.4	126.40
$\langle T \rangle$ (mK)	1660.4	1658	1660	
$\langle V \rangle$ (mK)	-1786.8	-1785	-1787	
$\sqrt{\langle r_{ij}^2 \rangle}$ (Å)	10.96	10.95	10.96	
$\langle r_{ij} \rangle$ (Å)	9.616	9.612	9.610	
$\langle r_{ij}^{-1} \rangle$ (Å $^{-1}$)	0.134	0.135		
$\langle r_{ij}^{-2} \rangle$ (Å $^{-2}$)	0.0228	0.0230		
$\sqrt{\langle r_{iG}^2 \rangle}$ (Å)	6.326		6.49	6.32
$C_3^{(0)}$ (Å $^{-\frac{1}{2}}$)	0.562		0.567	
trimer	excited state			
	present	Ref.[25]	Ref.[26]	Ref.[27]
$B_3^{(1)}$ (mK)	2.2706	2.268	2.265	2.2707
$\langle T \rangle$ (mK)	122.15	122.1	121.9	
$\langle V \rangle$ (mK)	-124.42	-124.5	-124.2	
$\sqrt{\langle r_{ij}^2 \rangle}$ (Å)	104.5	104.3	101.9	
$\langle r_{ij} \rangle$ (Å)	84.51	83.53	83.08	
$\langle r_{ij}^{-1} \rangle$ (Å $^{-1}$)	0.0265	0.0267		
$\langle r_{ij}^{-2} \rangle$ (Å $^{-2}$)	0.00216	0.00218		
$\sqrt{\langle r_{iG}^2 \rangle}$ (Å)	60.33		58.8	59.3
$C_3^{(1)}$ (Å $^{-\frac{1}{2}}$)	0.179		0.178	

E. Trimer bound states

We calculated the wave functions of the trimer ground state, $\Psi_3^{(0)}$, and the excited state, $\Psi_3^{(1)}$, and their binding energies, $B_3^{(0)}$ and $B_3^{(1)}$, respectively, as well as some mean values with the $\Psi_3^{(v)}$ ($v = 0, 1$). Some of results are summarized in Table I together with those obtained in the literature. Our results excellently agree with those by Refs.[25-27]. The ^4He - ^4He bond length in the trimer ground state was measured as $\langle r_{ij} \rangle = 11_{-5}^{+4}$ Å [10], which is well explained by the calculations, $\langle r_{ij} \rangle = 9.61$ Å.

Those converged results were given by taking the symmetric three-body basis function $\{\Phi_\alpha^{(\text{sym})}; \alpha = 1, \dots, \alpha_{\text{max}}\}$ with $\alpha_{\text{max}} = 4400$, in which the shortest-range set is ($x_1 = 0.3$ Å, $y_1 = 0.4$ Å) and the longest-range one is ($x_{\text{max}} = 150$ Å, $y_{\text{max}} = 600$ Å). All the nonlinear parameters of the Gaussian basis set are listed in Table II.

TABLE II: All the nonlinear parameters of the Gaussian basis functions used for the ${}^4\text{He}$ -trimer states with $J = 0$ ($l_x = l_y$). Those in column a) are commonly for $\phi_{n_x l_x}^{(\cos)}(x)$ and $\phi_{n_x l_x}^{(\sin)}(x)$ and b) for $\psi_{n_y l_y}(y)$. Total number of the basis, α_{\max} , is 4400.

a) $\phi_{n_x l_x}^{(\cos)}(x), \phi_{n_x l_x}^{(\sin)}(x)$					b) $\psi_{n_y l_y}(y)$				number of basis
l_x	n_x^{\max}	x_1 [Å]	$x_{n_x^{\max}}$ [Å]	ω	l_y	n_y^{\max}	y_1 [Å]	$y_{n_y^{\max}}$ [Å]	
0	22	0.3	150.0	1.0	0	50	0.4	600.0	2200
2	17	0.6	150.0	1.0	2	40	0.8	400.0	1360
4	14	0.8	130.0	1.0	4	30	1.0	200.0	840

There are neither additional parameter nor assumptions. The present calculation is so transparent that it is possible for the readers to repeat the calculation and check the results reported here. The parameters for the Gaussian ranges are in round numbers but further optimization of them do not improve the binding energies ($B_3^{(0)} = 126.40$ mK and $B_3^{(1)} = 2.2706$ mK) as long as we calculate them with *five* significant figures (cf. another check in Sec.II.H about the accuracy of the calculation).

Convergence of the binding energies $B_3^{(0)}$ and $B_3^{(1)}$ with respect to increasing partial waves $l_x (= l_y)$ is shown in Table III in comparison with the Faddeev calculation by Lazauskas and Carbonell [25]. The case $l_{x_{\max}} = 4$ is sufficient in the present work as long as the accuracy of five significant digits is required.

The convergence of the present result is more rapid than that of the Faddeev solution (the same will be seen in the tetramer calculation in Sec.III). The reason is that both the interaction and the wave function are truncated in the angular-momentum space (l_{\max}) in the Faddeev calculations, but the full interaction is included in the present calculation (with no partial-wave decomposition) though the wave function is truncated (l_{\max}). The difference of the convergence in the two calculation methods was precisely discussed in the case of the three nucleon bound states (${}^3\text{H}$ and ${}^3\text{He}$ nuclei) in our GEM calculation [41–43] and in a Faddeev calculation [53]; for an illustration of the difference, see Fig. 15 in Ref. [43]. In this context, it is worth pointing out that, in Table I, our result precisely agrees with another Faddeev calculation by Ref.[27] with no the partial wave decomposition.

Use of the value $\frac{\hbar^2}{m} = 12.11928 \text{ K}\text{\AA}^2$ [52] results in $B_3^{(0)} = 126.499$ mK and $B_3^{(1)} = 2.27787$ mK, while Ref. [52] gives 126.499 mK and 2.27844 mK, respectively. Calculation of the binding energy was also made perturbatively with $B_3 = \frac{12.11928}{12.12} \langle T \rangle + \langle V \rangle$, where $\langle T \rangle$ and $\langle V \rangle$ are those obtained with $\frac{\hbar^2}{m} = 12.12 \text{ K}\text{\AA}^2$; this gives $B_3^{(0)} = 126.498$ mK and $B_3^{(1)} = 2.27787$ mK. The calculations below in Sec.II.F-H take $\frac{\hbar^2}{m} = 12.12 \text{ K}\text{\AA}^2$.

TABLE III: Convergence of the ${}^4\text{He}$ trimer calculations with respect to the increasing maximum partial wave (l_{\max}). The four columns present trimer ground ($B_3^{(0)}$) and excited ($B_3^{(1)}$) state energies in comparison with those obtained by the Faddeev-equation calculation of Ref.[25].

trimer l_{\max}	present		Ref.[25]	
	$B_3^{(0)}$ (mK)	$B_3^{(1)}$ (mK)	$B_3^{(0)}$ (mK)	$B_3^{(1)}$ (mK)
0	121.00	2.2397	89.01	2.0093
2	126.39	2.2705	120.67	2.2298
4	126.40	2.2706	125.48	2.2622
8			126.34	2.2677
12			126.39	2.2680
14			126.39	2.2680

F. Short-range correlation and asymptotic behavior

In order to see how the present method describes the short-range structure of trimer, we calculated the pair correlation function (pair distribution function or two-body density) $P_3^{(v)}(x)$ defined by

$$P_3^{(v)}(x_1) Y_{00}(\hat{\mathbf{x}}_1) = \langle \Psi_3^{(v)} | \Psi_3^{(v)} \rangle_{\mathbf{y}_1}, \quad (2.23)$$

where the symbol $\langle \rangle_{\mathbf{y}_1}$ means the integration over \mathbf{y}_1 only. This integration gives an analytical expression owing to the use of the Gaussian basis functions; here, we explicitly rewrite $\Psi_3^{(v)}$ as a function of $(\mathbf{x}_1, \mathbf{y}_1)$ by transforming the other coordinates $(\mathbf{x}_2, \mathbf{y}_2)$ and $(\mathbf{x}_3, \mathbf{y}_3)$ into $(\mathbf{x}_1, \mathbf{y}_1)$. $P_3^{(v)}(x_i)$ is independent of i ($= 1, 2, 3$) and is apparently normalized as $\int P_3^{(v)}(x) x^2 dx = 1$. It presents the probability of finding two particles at an interparticle distance x .

In Fig. 3, short-range structure of $P_3^{(v)}(x)$ ($v = 0, 1$) is illustrated together with $P_2(x)$ ($= |\Psi_2(x)|^2$) for the ${}^4\text{He}$ dimer. The dashed line is for the trimer ground state ($v = 0$). The solid line for the excited state ($v = 1$) and the dotted line for the dimer have been multiplied by factors 14.5 and 6.0, respectively. It is of interest that precisely the same shape of the short-range correlation ($x \lesssim 4 \text{ \AA}$) as seen in the dimer appears both in the trimer ground and excited states (the same will be seen in the tetramer ground and excited states in the next section). This gives a foundation to an *a priori* assumption that a two-particle correlation function (such as the Jastrow function) to simulate the short-range part of the dimer radial wave function $\Psi_2(x)$ is incorporated in the three-body wave function from the beginning.

To investigate the trimer configuration in the asymptotic region where one atom is far from the other two,

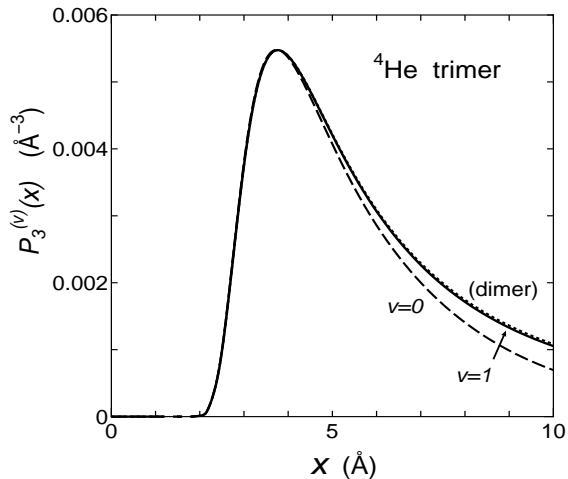


FIG. 3: Short-range structure of the pair correlation function $P_3^{(v)}(x)$ of the ${}^4\text{He}$ trimer calculated by (2.23). The dashed line is for the trimer ground state ($v = 0$), the solid line for the excited state ($v = 1$) and the dotted line for the ${}^4\text{He}$ dimer ($|\Psi_2(x)|^2$). The solid and dotted lines have been multiplied by factors 14.5 and 6.0, respectively, to be normalized at the peak. The same shape of the short-range correlation ($x \lesssim 4$ Å) appears in the three states.

we calculate the overlap function $\mathcal{O}_3^{(v)}(y_1)$ [26, 41, 46–48] to describe the overlap between the trimer wave function $\Psi_3^{(v)}(v = 0, 1)$ and the dimer one $\Psi_2(\mathbf{x})$:

$$\mathcal{O}_3^{(v)}(y_1) Y_{00}(\hat{\mathbf{y}}_1) = \langle \Psi_2(\mathbf{x}_1) | \Psi_3^{(v)} \rangle_{\mathbf{x}_1}. \quad (2.24)$$

In Fig. 4, we plot $y \mathcal{O}_3^{(v)}(y)$ for the ground and excited states. They should asymptotically satisfy

$$y \mathcal{O}_3^{(v)}(y) \xrightarrow{y \rightarrow \infty} C_3^{(v)} \exp(-\kappa_3^{(v)} y), \quad (2.25)$$

where $\kappa_3^{(v)}$ is the binding wave number given by $\kappa_3^{(v)} = \sqrt{2\mu_y(B_3^{(v)} - B_2)}/\hbar$ ($\kappa_3^{(0)} = 0.117$ Å $^{-1}$, $\kappa_3^{(1)} = 0.0103$ Å $^{-1}$). The amplitude $C_3^{(v)}$ is called the asymptotic normalization coefficient (ANC) [26, 41, 46–48] defining the amplitude of the tail of the radial overlap function. The asymptotic functions (2.25) with $C_3^{(0)} = 0.562$ Å $^{-\frac{1}{2}}$ and $C_3^{(1)} = 0.179$ Å $^{-\frac{1}{2}}$ (see the open circles) are precisely reproduced by the dashed line ($v = 0$) and the solid line ($v = 1$), respectively, up to $y \sim 1000$ Å, which demonstrates the accuracy of our wave functions in the asymptotic region. The values of $C_3^{(v)}$ agree with those given by Barletta and Kievsky [26] using a variational method with correlated hyperspherical harmonics functions (see Table I).

The total three-body wave function $\Psi_3^{(v)}(v = 0, 1)$ is represented asymptotically as

$$\Psi_3^{(v)} \longrightarrow C_3^{(v)} \sum_{i=1}^3 \Psi_2(\mathbf{x}_i) \frac{e^{-\kappa_3^{(v)} y_i}}{y_i} Y_{00}(\hat{\mathbf{y}}_i). \quad (2.26)$$

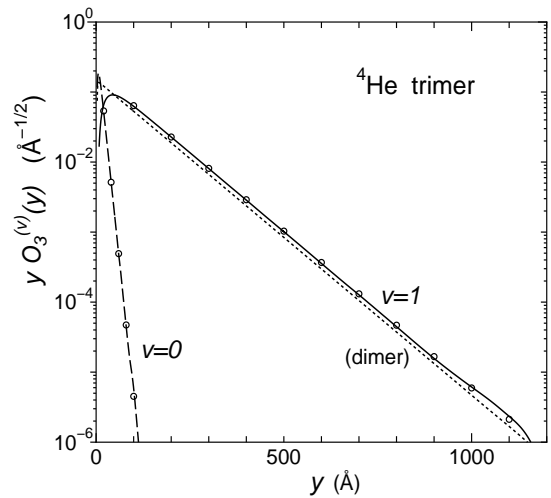


FIG. 4: Overlap function $\mathcal{O}_3^{(v)}(y)$, multiplied by y , between the ${}^4\text{He}$ trimer wave function ($v = 0, 1$) and the dimer one, which is defined by (2.24). Open circles represent the fit of the asymptotic function (2.25) to $\mathcal{O}_3^{(v)}(y)$ using the asymptotic normalization coefficient $C_3^{(v)}$. The solid line ($v = 1$) is found to be parallel to the dotted line for the dimer wave function ($y \Psi_2(y)$).

The ANC, $C_3^{(v)}$, is a quantity to convey the interior structural information of the trimer to the asymptotic behavior. It is known, in the nuclear peripheral reactions where only the asymptotic tails of the wave functions of reacting particles contribute to the reaction process, the cross section is proportional to the squared ANC which can be measured in some specific systems [47, 48, 54]. The idea of ANC might be available to the calculation of ${}^4\text{He}$ atoms reactions such as dimer + dimer \rightarrow trimer + atom. Also, attention to the ANC might be useful when one intends to reproduce the non-universal variations of the trimer states by parametrizing effective models.

G. 'Dimerlike-pair' model in asymptotic region

In Fig. 4, we find that the solid line ($v = 1$) is parallel to the dotted line (dimer); namely, $\kappa_3^{(1)} (= 0.0103$ Å $^{-1})$ is very close to $\kappa_2 (= 0.0104$ Å $^{-1})$. This agreement is not accidental, but is understandable from a model, which we refer to as a 'dimerlike-pair' model, for the asymptotic behavior of the trimer excited state (Fig. 5a). The model tells that i) particle a , located far from b and c which are *loosely* bound (dimer), is little affected by the interaction between b and c , ii) therefore, the pair a and b at a distance x is asymptotically dimerlike, iii) since $\mathbf{x} \simeq \mathbf{y}$ asymptotically, the amplitude of particle a along \mathbf{y} is dimerlike, namely $\kappa_3^{(1)} \simeq \kappa_2$.

If this model is acceptable, we can predict that, in the asymptotic region, the pair correlation function of the trimer excited state, $x^2 P_3^{(1)}(x)$, should decay ex-

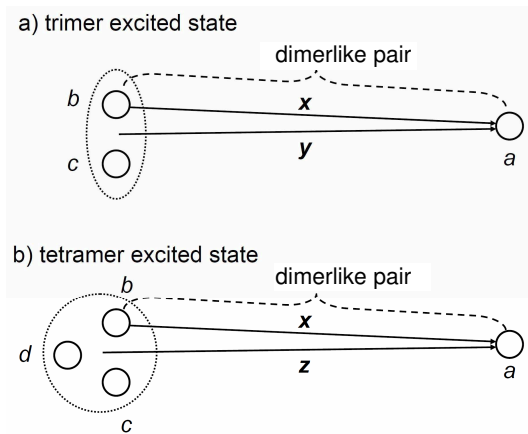


FIG. 5: 'Dimerlike-pair' model for the asymptotic behavior of the trimer and tetramer excited states (see text).

ponentially with the same rate as that in the dimer ($x^2 P_2(x)$). This is clearly seen in Fig. 6; the solid and dotted lines have almost the same exponentially-decaying rate of $2\kappa_3^{(1)}$ ($\simeq 2\kappa_2$). The same evidence is seen in Figs. 3 and 14 of our previous calculation of the ^4He trimer using the HFDHE2 potential reported in Ref. [43].

Once we accept the dimerlike-pair model ($\kappa_3^{(1)} \simeq \kappa_2$), we can estimate $B_3^{(1)}$, the trimer excited-state binding energy, using B_2 . With the use of the definitions of the binding wave numbers:

$$\kappa_2 = \sqrt{2\mu_x B_2}/\hbar, \quad (2.27)$$

$$\kappa_3^{(1)} = \sqrt{2\mu_y (B_3^{(1)} - B_2)}/\hbar, \quad (2.28)$$

where $\mu_x = \frac{1}{2}m$ and $\mu_y = \frac{2}{3}m$. Taking $\kappa_3^{(1)} \simeq \kappa_2$, we can then predict

$$B_3^{(1)} \simeq B_2 + \frac{\mu_x}{\mu_y} B_2 = \frac{7}{4} B_2 = 2.281 \text{ mK}, \quad (2.29)$$

which is close to 2.2706 mK by the present three-body calculation using the LM2M2 potential for which we have the ratio $B_3^{(1)}/B_2 = 1.74$ ($\simeq 7/4$).

In order to see a deviation of the ratio from 7/4 depending on the realistic potentials in the literature, we refer to $B_3^{(1)}/B_2 = 1.59$ [26] (SAPT2 [8]), 1.65 [39, 52] (SAPT2007 [9]), 1.74 [26, 27] (TTY [7]), 1.74 (LM2M2), 2.01 [37] (HFDHE2). The dimerlike-pair model provides a reason why the ratio $B_3^{(1)}/B_2$ is located around 7/4 in a narrow region of 1.6–2.0.

We note that this model should be considered under the condition that the ^4He atoms are interacting with a realistic pair potential and should not be discussed in any situation where a large deformation of the strength is posed to the potential (cf. a discussion in Sec.III of Ref. [13] on the Efimov states in ^4He trimer).

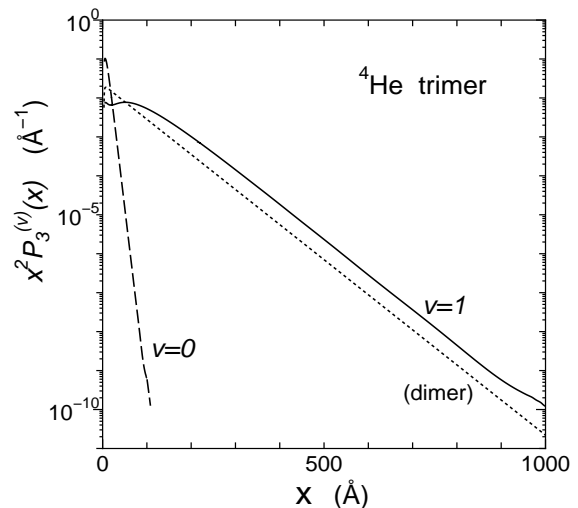


FIG. 6: Asymptotic behavior of the pair correlation (distribution) function $P_3^{(v)}(x)$, multiplied by x^2 , of the ^4He trimer. The dashed line is for the trimer ground state ($v=0$). The solid line for the excited state ($v=1$) and the dotted line for the dimer are found to have almost the same exponentially-decaying rate, $2\kappa_3^{(1)} \simeq 2\kappa_2$.

We try to apply the same model to the tetramer excited state (Fig. 5b) and predict its binding energy $B_4^{(1)}$. Asymptotically, particle a decays from the trimer ($b+c+d$) as $\exp(-\kappa_4^{(1)}z)$ with

$$\kappa_4^{(1)} = \sqrt{2\mu_z (B_4^{(1)} - B_3^{(0)})}/\hbar, \quad (2.30)$$

where $\mu_z = \frac{3}{4}m$ is the reduce atom-trimer mass. Taking $\kappa_4^{(1)} \simeq \kappa_2$, we predict $B_4^{(1)}$ as

$$B_4^{(1)} \simeq B_3^{(0)} + \frac{\mu_x}{\mu_z} B_2 = B_3^{(0)} + \frac{2}{3} B_2 = 127.27 \text{ mK} \quad (2.31)$$

when employing the calculated values of $B_3^{(0)}$ and B_2 with LM2M2. In Sec.III, we make a four-body calculation of the tetramer with LM2M2 and check the above prediction of $B_4^{(1)}$.

H. Generalized eigenvalue problem

In this subsection, we discuss about a technical subject on a numerical trouble which arises when solving the generalized eigenvalue problem (2.6). This is due to the fact that the overlap matrix \mathcal{N} becomes almost singular when a very large number of nonorthogonal basis functions $\{\Phi_\alpha^{(\text{sym})}\}$ employed. In this case, because of the non-negligible round-off error in double-precision computation ($\simeq 16$ decimal digits), we may obtain no solution of (2.6) or a solution that includes some unphysically too

deep erroneous bound state. In order to overcome this trouble, we took the following two steps:

Step i): we first diagonalize the overlap matrix \mathcal{N} :

$$\sum_{\alpha'=1}^{\alpha_{\max}} \mathcal{N}_{\alpha,\alpha'} C_{\alpha'}^{(N)} = \nu_N C_{\alpha}^{(N)}, \quad (2.32)$$

where $\alpha, N = 1, \dots, \alpha_{\max}$. The eigenvalues ν_N are positive definite since $\mathcal{N}_{\alpha,\alpha'} = \mathcal{N}_{\alpha',\alpha}$. We then define a new, symmetrized *orthonormal* basis set:

$$\widehat{\Phi}_N^{(\text{sym})} = \frac{1}{\sqrt{\nu_N}} \sum_{\alpha=1}^{\alpha_{\max}} C_{\alpha}^{(N)} \Phi_{\alpha}^{(\text{sym})}, \quad (2.33)$$

$$\langle \widehat{\Phi}_N^{(\text{sym})} | \widehat{\Phi}_{N'}^{(\text{sym})} \rangle = \delta_{N,N'}, \quad (2.34)$$

where $N, N' = 1, \dots, \alpha_{\max}$. The generalized eigenvalue problem (2.6) are then equivalently converted into a standard eigenvalue problem:

$$\sum_{N'=1}^{\alpha_{\max}} [\widehat{\mathcal{H}}_{N,N'} - E \delta_{N,N'}] \widehat{A}_{N'} = 0, \quad (2.35)$$

where $N = 1, \dots, \alpha_{\max}$, and

$$\widehat{\mathcal{H}}_{N,N'} = \langle \widehat{\Phi}_N^{(\text{sym})} | H | \widehat{\Phi}_{N'}^{(\text{sym})} \rangle. \quad (2.36)$$

Here, we arrange $\{\widehat{\Phi}_N^{(\text{sym})}\}$ in the decreasing order of ν_N :

$$\nu_1 > \nu_2 > \dots > \nu_N > \dots > \nu_{\alpha_{\max}}. \quad (2.37)$$

When the nonorthogonality among the basis functions $\{\Phi_{\alpha}^{(\text{sym})}\}$ is very large, some of ν_N become extremely small and therefore the large factor $1/\sqrt{\nu_N}$ may cause a serious cancellation in the summation in (2.33). Since the present calculation is performed by double-precision computation, such a large cancellation may generate a substantial round-off error in (2.33) and hence in the matrix elements (2.36). This may give rise to some erroneous eigenstates in (2.35) that have unphysically huge binding energies.

Step ii): We therefore omit such members of $\{\widehat{\Phi}_N^{(\text{sym})}\}$ that have too small ν_N . The binding energies of such unphysical states decreases quickly as the basis size is reduced. Finally, we reach an appropriate size, say \widehat{N}_{\max} , of the basis $\{\widehat{\Phi}_N^{(\text{sym})}\}$ for which those unphysical states have disappeared from the low-energy region, and energies of the lowest-lying (deepest) states take physically reasonable values. It is to be emphasized that the binding energies of so-obtained lowest-lying physical states are stable against further reduction of \widehat{N}_{\max} .

Table IV explicitly demonstrates *Step ii)*. We start with $\alpha_{\max} = 4400$ basis functions $\{\Phi_{\alpha}^{(\text{sym})}\}$ whose parameters are given in Table II. When the size of the new basis $\{\widehat{\Phi}_N^{(\text{sym})}\}$ is reduced from α_{\max} to $\widehat{N}_{\max} = 3250$ according to (2.37), the solution of (2.35) has come to include no unphysical state and give the binding energies $B_3^{(0)} = 126.3999$ mK and $B_3^{(1)} = 2.270606$ mK for

TABLE IV: Stability of the calculated trimer binding energies of the lowest-lying two states against decreasing number (\widehat{N}_{\max}) of symmetrized orthonormal three-body basis functions $\{\widehat{\Phi}_N^{(\text{sym})}\}$ of Eq.(2.33). This assures accuracy of the conclusion $B_3^{(0)} = 126.40$ mK and $B_3^{(1)} = 2.2706$ mK in Table I.

\widehat{N}_{\max}	$(\Delta\widehat{N}_{\max})$	$B_3^{(0)}$ (mK)	$B_3^{(1)}$ (mK)
3250	–	126.3999	2.270606
3240	(–10)	126.3998	2.270605
3200	(–50)	126.3995	2.270602
3150	(–100)	126.3991	2.270594
2950	(–300)	126.3975	2.270533
2750	(–500)	126.3954	2.270484
2250	(–1000)	126.3657	2.270163

the lowest two states. By checking the stability of the energy values against further decreasing \widehat{N}_{\max} , we verify the values of $B_3^{(0)} = 126.40$ mK and $B_3^{(1)} = 2.2706$ mK in Table I.

III. ${}^4\text{He}$ TETRAMER

Calculation of the ${}^4\text{He}$ tetramer using realistic potentials has been performed in Refs. [25, 28–31]. Although binding energy of the ground state obtained in the papers agrees well with each other (~ 558 mK), that of the loosely bound excited state differs significantly from each other; namely, the binding energy with respect to the trimer ground state (126.4 mK) is given as 1.1 mK by the Faddeev-Yakubovski (FY) equations method [25], 6.6 mK by Monte Carlo methods combined with the adiabatic hyperspherical approximation [30] and 52 mK recently by using a method of the correlated potential harmonic basis functions [31]. Though the Faddeev result (1.1 mK) seems to the present authors the most accurate, the excited state was not solved as a bound-state problem in Ref. [25] but the result was extrapolated from the atom-trimer scattering phase shifts.

Thus the purpose of this section is to perform, using the same LM2M2 potential as in Ref. [25], accurate bound-state calculation of the tetramer excited state, not only giving a precise binding energy but also describing the short-range correlation and the asymptotic behavior of the wave function properly.

The GEM has extensively been employed in bound-state calculations of various four-body systems in nuclear and hypernuclear physics (cf. review papers [43–45]). Extension from three-body GEM calculations to four-body ones in the presence of strong short-range repulsion is a familiar subject in nuclear physics. For example, the study of three-nucleon bound states (${}^3\text{H}$ and ${}^3\text{He}$

nuclei) in Ref. [41] was extended to that of four-nucleon ground state (${}^4\text{He}$ nucleus, $J^\pi = 0^+$) [55] and the first excited, very diffuse state ($J^\pi = 0^+$) [56]. The study of the three- α -particle system (${}^{12}\text{C}$ nucleus) [43, 57, 58] was extended to that of the four- α -particle system (${}^{16}\text{O}$ nucleus) [58] with the strongly repulsive Pauli-blocking projection operator on the α - α motion. Therefore, extension of the ${}^4\text{He}$ trimer calculation to the tetramer one is straightforward on account of those experiences.

A. Method

We take two types of Jacobi coordinate sets, K-type and H-type (Fig. 7). Namely, for K-type, $\mathbf{x}_1 = \mathbf{r}_2 - \mathbf{r}_1$, $\mathbf{y}_1 = \mathbf{r}_3 - \frac{1}{2}(\mathbf{r}_1 + \mathbf{r}_2)$ and $\mathbf{z}_1 = \mathbf{r}_4 - \frac{1}{3}(\mathbf{r}_1 + \mathbf{r}_2 + \mathbf{r}_3)$ and cyclically for $\{\mathbf{x}_i, \mathbf{y}_i, \mathbf{z}_i; i = 2, \dots, 12\}$ by the symmetrization between the four particles. For H-type, $\mathbf{x}_{13} = \mathbf{r}_2 - \mathbf{r}_1$, $\mathbf{y}_{13} = \mathbf{r}_4 - \mathbf{r}_3$, $\mathbf{z}_{13} = \frac{1}{2}(\mathbf{r}_3 + \mathbf{r}_4) - \frac{1}{2}(\mathbf{r}_1 + \mathbf{r}_2)$ and cyclically for $\{\mathbf{x}_i, \mathbf{y}_i, \mathbf{z}_i; i = 14, \dots, 18\}$. An explicit illustration of the totally 18 sets of the rearrangement Jacobi coordinates of four-body systems is seen in Fig. 18 of Ref. [43].

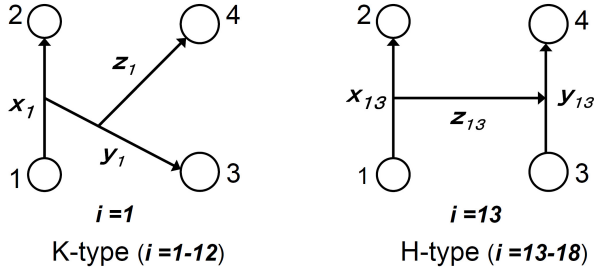


FIG. 7: Jacobi coordinates, K-type and H-type, for the ${}^4\text{He}$ tetramer. Symmetrization of the four particles generates the sets $i = 1, \dots, 12$ (K-type) and $i = 13, \dots, 18$ (H-type).

The total four-body wave function Ψ_4 is to be obtained by solving the Schrödinger equation

$$(H - E)\Psi_4 = 0 \quad (3.1)$$

with the Hamiltonian

$$H = -\frac{\hbar^2}{2\mu_x}\nabla_x^2 - \frac{\hbar^2}{2\mu_y}\nabla_y^2 - \frac{\hbar^2}{2\mu_z}\nabla_z^2 + \sum_{1 \leq i < j}^4 V(r_{ij}), \quad (3.2)$$

where $\mu_x = \frac{1}{2}m$, $\mu_y = \frac{2}{3}m$ and $\mu_z = \frac{3}{4}m$ on the K-type coordinates, and $\mu_x = \mu_y = \frac{1}{2}m$ and $\mu_z = m$ on the H-type ones.

Ψ_4 is expanded in terms of the symmetrized L^2 -integrable K-type and H-type four-body basis functions:

$$\Psi_4 = \sum_{\alpha_K=1}^{\alpha_K^{\max}} A_{\alpha_K}^{(K)} \Phi_{\alpha_K}^{(\text{sym};K)} + \sum_{\alpha_H=1}^{\alpha_H^{\max}} A_{\alpha_H}^{(H)} \Phi_{\alpha_H}^{(\text{sym};H)}, \quad (3.3)$$

with

$$\Phi_{\alpha_K}^{(\text{sym};K)} = \sum_{i=1}^{12} \Phi_{\alpha_K}^{(K)}(\mathbf{x}_i, \mathbf{y}_i, \mathbf{z}_i), \quad (3.4)$$

$$\Phi_{\alpha_H}^{(\text{sym};H)} = \sum_{i=13}^{18} \Phi_{\alpha_H}^{(H)}(\mathbf{x}_i, \mathbf{y}_i, \mathbf{z}_i), \quad (3.5)$$

in which $\Phi(\mathbf{x}_i, \mathbf{y}_i, \mathbf{z}_i)$ is a function of i -th set of Jacobi coordinates. It is of importance that $\Phi_{\alpha_K}^{(\text{sym};K)}$ and $\Phi_{\alpha_H}^{(\text{sym};H)}$ are constructed on the full 18 sets of Jacobi coordinates; this makes the function space of the basis quite wide.

The eigenenergies E and amplitudes $A_{\alpha_K}^{(K)}$ ($A_{\alpha_H}^{(H)}$) are determined by the Rayleigh-Ritz variational principle:

$$\langle \Phi_{\alpha_K}^{(\text{sym};K)} | H - E | \Psi_4 \rangle = 0, \quad (3.6)$$

$$\langle \Phi_{\alpha_H}^{(\text{sym};H)} | H - E | \Psi_4 \rangle = 0, \quad (3.7)$$

where $\alpha_K = 1, \dots, \alpha_K^{\max}$ and $\alpha_H = 1, \dots, \alpha_H^{\max}$. This set of equations results in a generalized eigenvalue problem:

$$\sum_{c'=K,H} \sum_{\alpha_{c'}=1}^{\alpha_{c'}^{\max}} \left[\mathcal{H}_{\alpha_c, \alpha_{c'}}^{(c, c')} - E \mathcal{N}_{\alpha_c, \alpha_{c'}}^{(c, c')} \right] A_{\alpha_{c'}}^{(c')} = 0, \quad (3.8)$$

where $c = K, H$ and $\alpha_c = 1, \dots, \alpha_c^{\max}$. The matrix elements are given by

$$\mathcal{H}_{\alpha_c, \alpha_{c'}}^{(c, c')} = \langle \Phi_{\alpha_c}^{(c)} | H | \Phi_{\alpha_{c'}}^{(c')} \rangle, \quad (3.9)$$

$$\mathcal{N}_{\alpha_c, \alpha_{c'}}^{(c, c')} = \langle \Phi_{\alpha_c}^{(c)} | 1 | \Phi_{\alpha_{c'}}^{(c')} \rangle. \quad (3.10)$$

Up to here is the most general way of variational calculations for bound states of identical spinless four particles.

We describe the basis function $\Phi_{\alpha_K}^{(K)}$ ($\Phi_{\alpha_H}^{(H)}$) in the form

$$\begin{aligned} \Phi_{\alpha_K}^{(K)}(\mathbf{x}_i, \mathbf{y}_i, \mathbf{z}_i) &= \phi_{n_x l_x}^{(\cos)}(x_i) \phi_{n_y l_y}(y_i) \varphi_{n_z l_z}(z_i) \\ &\times \left[[Y_{l_x}(\hat{\mathbf{x}}_i) Y_{l_y}(\hat{\mathbf{y}}_i)]_{\Lambda} Y_{l_z}(\hat{\mathbf{z}}_i) \right]_{JM}, \\ &(i = 1, \dots, 12) \end{aligned} \quad (3.11)$$

$$\begin{aligned} \Phi_{\alpha_H}^{(H)}(\mathbf{x}_i, \mathbf{y}_i, \mathbf{z}_i) &= \phi_{n_x l_x}^{(\cos)}(x_i) \psi_{n_y l_y}(y_i) \varphi_{n_z l_z}(z_i) \\ &\times \left[[Y_{l_x}(\hat{\mathbf{x}}_i) Y_{l_y}(\hat{\mathbf{y}}_i)]_{\Lambda} Y_{l_z}(\hat{\mathbf{z}}_i) \right]_{JM}, \\ &(i = 13, \dots, 18) \end{aligned} \quad (3.12)$$

where α_K specifies a set

$$\alpha_K \equiv \{ \text{'cos' or 'sin'}, \omega, n_x l_x, n_y l_y, n_z l_z, \Lambda, JM \}, \quad (3.13)$$

which is commonly for the components $i = 1, \dots, 12$; and similarly for α_H commonly for $i = 13, \dots, 18$.

Since we consider the case of $J = 0$ in this paper, the totally symmetric four-body wave function requires i) $l_x = \text{even}$, $l_y + l_z = \text{even}$ and $\Lambda = l_z$ for the K-type basis and ii) $l_x = \text{even}$, $l_y = \text{even}$ and $\Lambda = l_z = \text{even}$ for the H-type basis.

In (3.11) and (3.12), the radial functions are assumed, as in Sec.II, to be

$$\phi_{n_x l_x}^{(\cos)}(x) = x^{l_x} e^{-(x/x_{n_x})^2} \times \left\{ \frac{\cos \omega(x/x_{n_x})^2}{\sin \omega(x/x_{n_x})^2} \right\}, \quad (3.14)$$

$$\psi_{n_y l_y}(y) = y^{l_y} e^{-(y/y_{n_y})^2}, \quad (3.15)$$

$$\varphi_{n_z l_z}(z) = z^{l_z} e^{-(z/z_{n_z})^2} \quad (3.16)$$

with geometric sequences of the Gaussian ranges:

$$x_{n_x} = x_1 a_x^{n_x - 1} \quad (n_x = 1, \dots, n_x^{\max}), \quad (3.17)$$

$$y_{n_y} = y_1 a_y^{n_y - 1} \quad (n_y = 1, \dots, n_y^{\max}), \quad (3.18)$$

$$z_{n_z} = z_1 a_z^{n_z - 1} \quad (n_z = 1, \dots, n_z^{\max}). \quad (3.19)$$

In (3.15), the 'cos(sin)'-type function is not adopted for $\psi_{n_y l_y}(y)$ of the H-type basis though y is the distance between two particles. This is because the 'cos(sin)'-type basis for the x -coordinate are applied to all the pairs of H-type by the symmetrization of the four particles.

In the tetramer calculation, the total number, $\alpha_{\max} = \alpha_K^{\max} + \alpha_H^{\max}$, of the symmetrized four-body basis functions (3.4) and (3.5) amounts to $\alpha_{\max} \sim 30000$, ranging from very compact to very diffuse, to obtain a well converged solution. Since the nonorthogonality among those basis functions is too large to solve directly the generalized eigenvalue problem (3.8), we take the same two-step method as described in Sec.II.H in the trimer calculation. We finally solve the same type of standard eigenvalue problem as (2.35) using the symmetric orthonormal four-body basis functions, $\{\widehat{\Phi}_N^{(\text{sym})}; N = 1, \dots, \widehat{N}_{\max}\}$, in which the basis with too small ν_N have been omitted.

B. Binding energy

In the calculation of the ^4He -tetramer ground state $\Psi_4^{(0)}$ and the excited state $\Psi_4^{(1)}$, the converged result was obtained by employing the symmetric four-body basis functions of $\alpha_{\max} = 29056$ with $l_{\max} = 4$. Table V shows the convergence of the binding energies of the tetramer ground ($B_4^{(0)}$) and excited ($B_4^{(1)}$) states with respect to increasing l_{\max} . Column 'K+H' is the result with both the K-type and H-type basis functions in (3.3), and column '(K)' is that with the K-type basis only.

Contribution from the K-type basis is dominant, but that from the H-type is sizable. Without the latter the excited state does not become bound ($B_4^{(1)} < B_3^{(0)} = 126.40$ mK) even for $l_{\max} = 4$. Since both type bases are not orthogonal to each other, the role of H-type one can be substituted in principle by the K-type one if a very large l_{\max} is employed. But, this is not practical; use of both types of bases is essentially important.

As seen in Table V, convergence of the binding energies with increasing l_{\max} is more rapid in our calculation than that in the FY-equations calculation [25]. The reason of this difference in the conversion is the same as that mentioned in the trimer calculation (Sec.II.E).

TABLE V: Convergence of ^4He tetramer calculations with respect to the increasing maximum partial wave (l_{\max}). $B_4^{(0)}$ and $B_4^{(1)}$ are the binding energies of the ground and excited states, respectively. Column 'K+H' is the results with both the K-type and H-type basis functions in (3.3) and column '(K)' is that with the K-type basis only. The excited state is unbound ($B_4^{(1)} < B_3^{(0)} = 126.40$ mK) in the cases denoted by the symbol '-'. For comparison, $B_4^{(0)}$ obtained by the FY-equations calculation [25] is listed in the last column. The LM2M2 potential is employed.

l_{\max}	tetramer				Ref.[25] $B_4^{(0)}$ (mK)
	present				
	$B_4^{(0)}$ (mK)	$B_4^{(1)}$ (mK)	$B_4^{(0)}$ (mK)	$B_4^{(1)}$ (mK)	
	K+H	(K)	K+H	(K)	
0	500.71	(185.96)	-	(-)	348.8
2	558.29	(508.62)	127.24	(-)	505.9
4	558.98	(532.56)	127.33	(-)	548.6
6					556.0
8					557.7

TABLE VI: Nonlinear parameters of the four-body Gaussian basis functions, (3.11)–(3.19), used for the ^4He tetramer ground and excited states with $J = 0$ ($\Lambda = l_z$) in the case of $l_{\max} = 2$ with 23504 basis functions (cf. Table V). In the leftmost column, K(H) stands for the K-type (H-type) basis. We take $\omega = 1.0$ in (3.14).

	$\phi_{n_x l_x}^{(\cos)}, \phi_{n_x l_x}^{(\sin)}$				$\psi_{n_y l_y}$				$\varphi_{n_z l_z}$			
	l_x	n_x^{\max}	x_1	$x_{n_x^{\max}}$	l_y	n_y^{\max}	y_1	$y_{n_y^{\max}}$	l_z	n_z^{\max}	z_1	$z_{n_z^{\max}}$
			[Å]	[Å]			[Å]	[Å]			[Å]	[Å]
K 0	14	0.2	20.0	0	15	0.8	50.0	0	20	0.8	400.0	
K 2	12	0.4	20.0	2	14	0.8	40.0	0	16	0.8	300.0	
K 0	8	0.3	6.0	2	8	0.8	6.0	2	8	1.0	6.0	
K 2	6	0.3	6.0	0	8	0.8	6.0	2	8	1.0	6.0	
K 0	8	0.3	6.0	1	8	0.8	6.0	1	8	1.0	6.0	
K 2	6	0.4	6.0	1	6	0.8	6.0	1	8	1.0	6.0	
K 2	6	0.5	6.0	2	8	0.8	6.0	2	8	1.0	6.0	
H 0	12	0.3	20.0	0	12	0.4	16.0	0	14	0.8	25.0	
H 2	6	0.6	6.0	2	6	0.8	6.0	0	8	1.0	6.0	
H 0	6	0.3	6.0	2	6	0.8	6.0	2	8	1.0	6.0	
H 2	6	0.6	6.0	0	6	0.8	6.0	2	8	1.0	6.0	
H 2	6	0.6	6.0	2	6	0.8	6.0	2	8	1.0	6.0	

In Table VI we list the nonlinear parameters of the four-body Gaussian basis functions, (3.11)–(3.19), in the

TABLE VII: Stability of the calculated binding energies of the ${}^4\text{He}$ tetramer ground and excited states with respect to the number (\widehat{N}_{max}) of the symmetrized orthonormal four-body basis functions corresponding to $\{\widehat{\Phi}_N^{(\text{sym})}\}$ in Eq.(2.33) in the case of $l_{\text{max}} = 4$ with the LM2M2 potential. This concludes $B_4^{(0)} = 558.98$ mK and $B_4^{(1)} = 127.33$ K.

\widehat{N}_{max}	$(\Delta\widehat{N}_{\text{max}})$	$B_4^{(0)}$ (mK)	$B_4^{(1)}$ (mK)
24800	–	558.983	127.326
24790	(–10)	558.981	127.326
24780	(–20)	558.980	127.326
24750	(–50)	558.977	127.326
24700	(–100)	558.975	127.325
24300	(–500)	558.954	127.323
23800	(–1000)	558.924	127.320

case of $l_{\text{max}} = 2$ with 23504 basis functions (cf. Table V) to avoid too long listing for $l_{\text{max}} = 4$. The range parameters are given in round numbers but further optimization of them do not improve the binding energies as long as we calculate them with five significant figures.

When solving the generalized eigenvalue problem (3.8), we take the same two-step method as mentioned in Sec.II.H. Table VII shows stability of the binding energies of the ground and excited states ($B_4^{(v)}, v = 0, 1$) against the decreasing number \widehat{N}_{max} of the symmetrized orthonormal four-body basis functions corresponding to $\{\widehat{\Phi}_N^{(\text{sym})}\}$ in Eq.(2.33).

Calculated binding energies and some of mean values of the tetramer ground and excited states are summarized in Table VIII(a) in comparison with those obtained by Lazauskas and Carbonell [25] with the FY-equations method in which the excited state was not obtained by a direct bound-state calculation but the binding energy (127.5 mK) was extrapolated from the atom-trimer scattering calculations. Our result of $B_4^{(1)} = 127.33$ mK, which is very closed to $B_4^{(1)}$ in Ref.[25], confirms the existence of the very shallow bound excited state ($J = 0$) of the ${}^4\text{He}$ tetramer. The tetramer excited state is located only by 0.93 mK below the trimer ground state (126.40 mK). This is analogous to that the trimer excited state lies by 0.967 mK below the dimer; a reason was explained in Sec.II.G by taking the dimerlike-pair model.

Table VIII(b) lists $B_4^{(0)}$ and $B_4^{(1)}$ obtained in other literature papers by the Monte Carlo methods [28–30] and by using the correlated potential harmonic basis [31]. All $B_4^{(0)}$ values agree well with the results by the present and FY-equations calculations, but $B_4^{(1)}$ by Refs. [30, 31] deviate significantly from our and FY-equations results.

Use of $\frac{\hbar^2}{m} = 12.11928 \text{ K}\text{\AA}^2$ [52] results in $B_4^{(0)} = 559.22$ mK and $B_4^{(1)} = 127.42$ mK. The same perturbative treat-

TABLE VIII: (a) Mean values of the ${}^4\text{He}$ tetramer ground and excited states calculated by the present work and the FY-equations method [25] with the use of the LM2M2 potential. B_4 is the binding energy, r_{ij} stands for interparticle distance and r_{iG} is the distance of a particle from the center-of-mass of the tetramer. (b) The other literature work [28–31] on the binding energies (see text). The values originally given in units of cm^{-1} are transformed in units of mK in the parentheses.

(a)				
tetramer	ground state		excited state	
	present	Ref.[25]	present	Ref.[25]
B_4 (mK)	558.98	557.7	127.33	127.5
$\langle T \rangle$ (mK)	4282.2	4107	1639.2	
$\langle V \rangle$ (mK)	–4841.2	–4665	–1766.5	
$\sqrt{\langle r_{ij}^2 \rangle}$ (\AA)	8.43	8.40	54.5	34.4
$\langle r_{ij} \rangle$ (\AA)	7.70		35.8	
$\langle r_{ij}^{-1} \rangle$ (\AA^{-1})	0.155		0.0792	
$\langle r_{ij}^{-2} \rangle$ (\AA^{-2})	0.0285		0.0117	
$\sqrt{\langle r_{iG}^2 \rangle}$ (\AA)	5.16		33.3	
$C_4^{(v)}$ ($\text{\AA}^{-\frac{1}{2}}$)	2.1		0.10	

(b)				
tetramer	Ref. [28]	Ref. [29]	Ref. [30]	Ref. [31]
$B_4^{(0)}$ (cm^{-1})	0.388(1)	0.3886(1)	0.387(1)	0.388
(mK)	(558)	(559.1)	(557)	(558)
$B_4^{(1)}$ (cm^{-1})			0.0922	0.124
(mK)			(133)	(178)

ment for the small difference of $\frac{\hbar^2}{m}$ as used in Sec.II.E gives $B_4^{(0)} = 559.23$ mK and $B_4^{(1)} = 127.42$ mK. The calculations below in Sec.III.C take $\frac{\hbar^2}{m} = 12.12 \text{ K}\text{\AA}^2$.

C. Short-range correlation and asymptotic behavior

Definition of the pair correlation function (2.23) for the trimer is extended to the tetramer states $\Psi_4^{(v)}(v = 0, 1)$:

$$P_4^{(v)}(x_1) Y_{00}(\widehat{\mathbf{x}}_1) = \langle \Psi_4^{(v)} | \Psi_4^{(v)} \rangle_{\mathbf{y}_1, \mathbf{z}_1}, \quad (3.20)$$

where $\langle \rangle_{\mathbf{y}_1, \mathbf{z}_1}$ means the integration over \mathbf{y}_1 and \mathbf{z}_1 .

The overlap function between a tetramer state $\Psi_4^{(v)}$ and a trimer one $\Psi_3^{(v_3)}(v_3 = 0, 1)$ is defined as a function of the atom-trimer distance z as an extension from (2.24):

$$\mathcal{O}_4^{(v_3, v)}(z_1) Y_{00}(\widehat{\mathbf{z}}_1) = \langle \Psi_3^{(v_3)} | \Psi_4^{(v)} \rangle_{\mathbf{x}_1, \mathbf{y}_1}. \quad (3.21)$$

All the integrals in (3.20) and (3.21) give the analytical expression owing to the use of Gaussian basis functions;

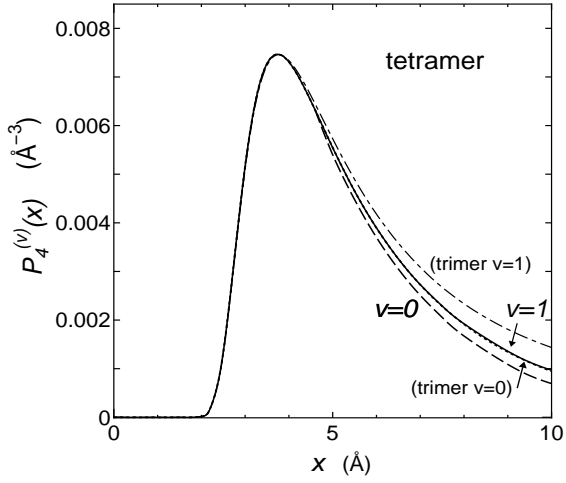


FIG. 8: Short-range structure of the pair correlation function $P_4^{(v)}(x)$ of the ^4He tetramer calculated by (3.20). The dashed line stands for the tetramer ground ($v=0$) state and the solid line for the excited ($v=1$) state. For the sake of comparison, additionally shown are the dotted line for the trimer ground state and the dash-dotted line for the trimer excited state. The solid, dotted and dash-dotted lines have been multiplied by factors 2.76, 1.36 and 19.8, respectively; the same shape of the short-range correlation ($x \lesssim 4 \text{ \AA}$) appears in all the states (cf. Fig. 3 for dimer).

$\Psi_4^{(v)}$ is to be transformed to a function of $(\mathbf{x}_1, \mathbf{y}_1, \mathbf{z}_1)$, and $\Psi_3^{(v_3)}$ to that of $(\mathbf{x}_1, \mathbf{y}_1)$.

In Fig. 8, we illustrate the short-range structure of the pair correlation functions $P_4^{(v)}(x)$ of the tetramer ground ($v=0$) and excited ($v=1$) states together with those of the trimer states. It is to be emphasized that the same shape of short-range correlation ($x \lesssim 4 \text{ \AA}$) appears in all the states (cf. Fig. 3 for the dimer) without introducing any pair correlation function.

The pair correlation functions $P_4^{(v)}(x)$ of the tetramer ($v=0, 1$) take very small values in the strongly-repulsive potential region ($x \lesssim 1.5 \text{ \AA}$) in Fig. 8; relative ratio of the values to the peak value is $\sim 10^{-6}$. This ratio is to be compared with $\sim 10^{-2}$ in the case of the four-nucleon bound state (^4He nucleus) calculated with a realistic nucleon-nucleon interaction with a strong short-range repulsion (the ratio is seen in Fig. 1 of Ref. [55] for the calculated pair correlation function of the ^4He nucleus). We understand that so strong is the repulsive core of the atom-atom potential.

In Fig. 9, we plot the overlap function $\mathcal{O}_4^{(v_3, v)}(z)$, multiplied by z , between the tetramer states ($v=0, 1$) and the trimer states ($v_3=0, 1$) in the region $z \leq 100 \text{ \AA}$. The two lines of $v=0, 1 (v_3=0)$ are to be compared with the result in Fig. 4 of Ref. [25] of the FY-equations calculation; the latter result represents the K-type FY components as a function of atom-trimer distance z . The two kinds of the results are resemble to each other though

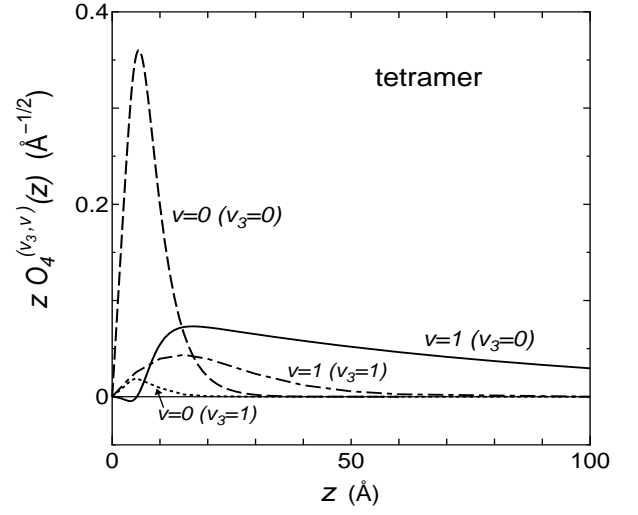


FIG. 9: Overlap function $\mathcal{O}_4^{(v_3, v)}(z)$ in (3.21), multiplied by z , between the trimer state ($v_3=0, 1$) and the tetramer state ($v=0, 1$) as a function of the atom-trimer distance z .

they do not stand for the same quantity. As for the excited state, the FY component is derived approximately by modifying the K-type FY amplitude of the zero-energy scattering [25]; the resulting amplitude is slightly more enhanced in the inner region than our overlap function of $v=1 (v_3=0)$. This is reflected in the r.m.s distance $\sqrt{\langle r_{ij}^2 \rangle}$ in Table VIII(a). In the plot of the overlap functions between the trimer *excited* state ($v_3=1$) and the tetramer states, it is reasonably seen that $\mathcal{O}_4^{(v_3=1, v)}(z)$ is much smaller than $\mathcal{O}_4^{(v_3=0, v)}(z)$ ($v=0, 1$) and decreases more rapidly along z .

In Fig. 10, $z \mathcal{O}_4^{(v_3=0, v)}(z)$ ($v=0, 1$) are illustrated in the asymptotic region. They should satisfy

$$z \mathcal{O}_4^{(v_3=0, v)}(z) \xrightarrow{z \rightarrow \infty} C_4^{(v)} \exp(-\kappa_4^{(v)} z) \quad (3.22)$$

with $\kappa_4^{(v)} = \sqrt{2\mu_z(B_4^{(v)} - B_3^{(0)})}/\hbar$ ($\kappa_4^{(0)} = 0.231 \text{ \AA}^{-1}$ and $\kappa_4^{(1)} = 0.0107 \text{ \AA}^{-1}$). The dashed line ($v=0$) and solid line ($v=1$) reproduces the asymptotic functions (3.22) with the ANC $C_4^{(0)} = 2.1 \text{ \AA}^{-\frac{1}{2}}$ and $C_4^{(1)} = 0.10 \text{ \AA}^{-\frac{1}{2}}$ (see the open circles), respectively, up to $y \sim 1000 \text{ \AA}$.

Asymptotically the tetramer is dissociated into the trimer ground state and a distant atom in the symmetric way between the four atoms (with negligible amount of the trimer excited state). Therefore, the tetramer wave function $\Psi_4^{(v)}$ ($v=0, 1$) is represented asymptotically as

$$\Psi_4^{(v)} \longrightarrow C_4^{(v)} \sum_{n=1}^4 \Psi_{3,n}^{(0)} \frac{e^{-\kappa_4^{(v)} z_n}}{z_n} Y_{00}(\hat{\mathbf{z}}_n), \quad (3.23)$$

where the summation over n symmetrizes the four atoms; namely, the n th atom is isolated at \mathbf{z}_n from the trimer

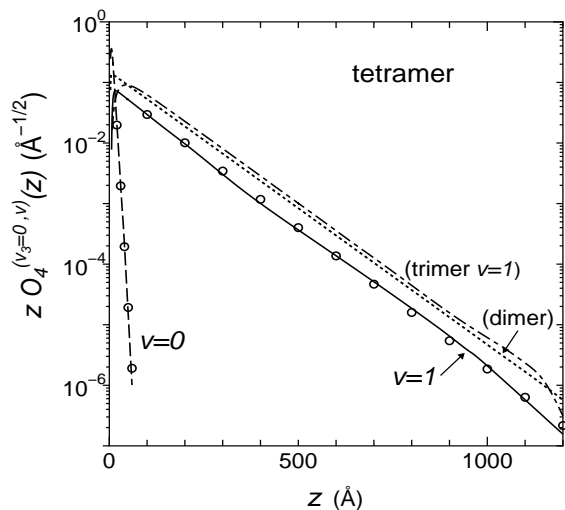


FIG. 10: Asymptotic behavior of the overlap function $\mathcal{O}_4^{(v_3=0,v)}(z)$, multiplied by z , between the trimer ground state ($v_3 = 0$) and the tetramer states ($v = 0, 1$). Open circles represent the fit of the asymptotic function (3.23) to $\mathcal{O}_4^{(v_3=0,v)}(z)$ using the asymptotic normalization coefficient $C_4^{(v)}$.

$\Psi_{3,n}^{(0)}$ in which the n th atom is absent and the other three atoms are symmetrized.

As for the tetramer's ANC, we can make the same comments as those for the trimer's ANC below Eq.(2.26).

D. 'Dimerlike-pair' model in asymptotic region

In Fig. 10, we note that the exponentially-decaying slope of the solid line ($\kappa_4^{(1)}$) is very close to that in the trimer excited state ($\kappa_3^{(1)}$) and that in the dimer (κ_2). This gives a support to the dimerlike-pair model for the tetramer excited state in the asymptotic region (Fig. 5b).

We can therefore predict that, in the asymptotic region, the pair correlation function $x^2 P_4^{(1)}(x)$ should be proportional to $\exp(-2\kappa_4^{(1)}x)$. This is seen in Fig. 11 though the solid line ($v = 1$) is not so excellently straight as in the trimer excited state (dot-dashed line) due to the complexity of the four-body calculation.

As mentioned in Sec.II.G, the dimerlike-pair model predicted $B_4^{(1)} \simeq 127.27$ mK. In the present calculation, we obtained $B_4^{(1)} = 127.33$ mK. The prediction is very good as long as the LM2M2 potential is employed.

Generally, in the case of ${}^4\text{He}_N$, the excited-state binding energy calculated using realistic potentials may be expected as

$$B_N^{(1)} \simeq B_{N-1}^{(0)} + \frac{N}{2(N-1)} B_2, \quad (3.24)$$

where the factor multiplied to B_2 comes from the ratio

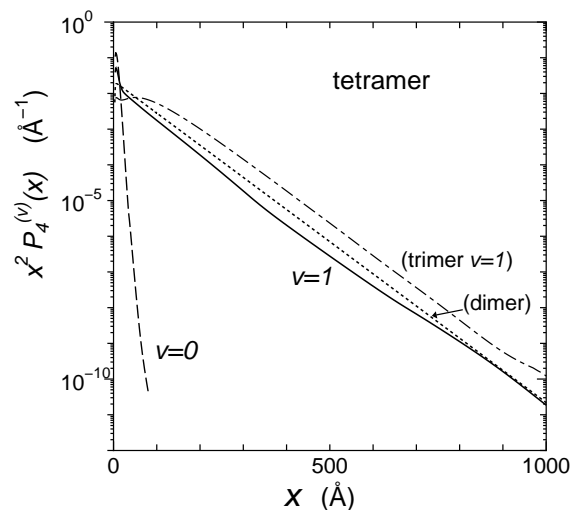


FIG. 11: Asymptotic behavior of the pair correlation function $P_4^{(v)}(x)$, multiplied by x^2 , of the ${}^4\text{He}$ tetramer calculated by (3.20). The dashed line stands for the tetramer ground ($v = 0$) state and the solid line for the excited ($v = 1$) state. The dotted line for the trimer excited state and the dotted line for the dimer are added for the sake of comparison.

of the reduced mass of the dimerlike pair ($\frac{1}{2}m$) to that of the ${}^4\text{He}-{}^4\text{He}_{N-1}$ system ($\frac{N-1}{N}m$). But, as discussed in Sec.II.G, the factor might depend on the realistic potentials with a small deviation (roughly ± 0.3).

IV. SUMMARY

We have calculated the ground and excited states of ${}^4\text{He}$ trimer and tetramer using the LM2M2 potential which has a strong short-range repulsive potential and is one of the most widely used ${}^4\text{He}-{}^4\text{He}$ interactions. We employed the Gaussian expansion method (GEM) for *ab initio* variational calculations of few-body systems. The symmetrized three-(four-)body Gaussian basis functions, ranging from very compact to very diffuse, are constructed on the full sets of possible Jacobi coordinates. Therefore, the basis set, spanning a wide function space, is suitable for describing both the short-range correlation (without assuming any pair correlation function) and the long-range asymptotic behavior of the trimer (tetramer) wave function as well as suitable for obtaining accurate binding energies. The main conclusions are summarized as follows:

i) Calculated binding energies of the trimer ground and excited states, $B_3^{(0)}$ and $B_3^{(1)}$, respectively, agree excellently with the literature (Table I); we have $B_3^{(0)} = 126.40$ mK and $B_3^{(1)} = 2.2706$ mK.

ii) As for the binding energies of the tetramer ground and excited states, we obtained $B_4^{(0)} = 558.98$ mK and $B_4^{(1)} = 127.33$ mK (situated only 0.93 mK below the

atom-trimer threshold). The former is in good agreement with the literature calculations, while the latter supports the result of 127.5 mK by Ref. [25] differently from the other literature results (Table VIII).

iii) We found that the strong short-range correlation ($r_{ij} \lesssim 4 \text{ \AA}$) seen in the dimer appears also in the ground and excited states of the trimer and tetramer precisely in the same shape (Figs. 3 and 8). This gives a foundation to an *a priori* assumption that a pair correlation function to simulate the short-range part of the dimer wave function is incorporated in the three-(four-)body wave function from the beginning.

iv) Illustrating the overlap function between the trimer excited state and the dimer ($\mathcal{O}_3^{(v=1)}$) and that between the tetramer excited state and the trimer ground state ($\mathcal{O}_4^{(v_3=0, v=1)}$), we found that those overlap functions are almost proportional to the dimer wave function in the asymptotic region up to $\sim 1000 \text{ \AA}$ (Figs. 4 and 10). Also it was found that the pair correlation functions of trimer and tetramer excited states ($P_3^{(v=1)}$ and $P_4^{(v=1)}$, respectively) are almost proportional to the squared dimer wave function in the asymptotic region (Figs. 6 and 11). We then came to propose a 'dimerlike pair' model (Fig. 5)

that predicts the excited-state binding energy of ${}^4\text{He}_N$ ($N \geq 3$) using Eq. (3.24). It will be of interest to examine this model in the case of $N \geq 5$. A five-body calculation of the pentamer, ${}^4\text{He}_5$, is in progress.

v) We calculated the asymptotic normalization coefficient (ANC) of the tail function of the dimer-atom (trimer-atom) relative motion in trimer (tetramer). This result may be available in peripheral reactions (insensitive to the interior of the system) including the ${}^4\text{He}$ trimers and tetramers, in which the reaction cross section will be proportional to the squared ANC. The ANC is a quantity to convey the interior structural information to the asymptotic behavior. Therefore, attention to this quantity might be helpful when one tries to reproduce the non-universal variation of the ${}^4\text{He}$ trimer (tetramer) states by means of parametrizing effective models beyond Efimov's universal theory.

Acknowledgement

The numerical calculations were performed on HITACHI SR16000 at KEK and YIFP.

-
- [1] V. Efimov, *Yad. Fiz.* **12**, 1080 (1970) [*Sov. J. Nucl. Phys.* **12**, 589 (1971)].
- [2] V. Efimov, *Nucl. Phys. A* **210**, 157 (1973).
- [3] V. Efimov, *Few-Body Syst.* **51**, 79 (2011).
- [4] F. Hoyle, *Astrophys. J. Suppl. Ser.* **1**, 121, (1954).
- [5] R.A. Aziz, V.P.S. Nain, J.S. Carley, W.L. Taylor and G.T. McConville, *J. Chem. Phys.* **70**, 4330 (1979).
- [6] R.A. Aziz and M.J. Slaman, *J. Chem. Phys.* **94**, 8047 (1991).
- [7] K.T. Tang, J.P. Toennies and C.L. Yiu, *Phys. Rev. Lett.* **74**, 1546 (1995).
- [8] A.R. Jansen and R.A. Aziz, *J. Chem. Phys.* **107**, 914 (1997).
- [9] M. Jeziorska, W. Cencek, K. Patkowski, B. Jeziorski and K. Szalewicz, *J. Chem. Phys.* **127**, 124303 (2007).
- [10] R. Grisenti *et al.*, *Phys. Rev. Lett.* **85**, 2284 (2000).
- [11] E.A. Kolganova, A.K. Motovilov and W. Sandhas, *Phys. Part. Nucl.* **40**, 206 (2009).
- [12] E.A. Kolganova, A.K. Motovilov and W. Sandhas, *Few-Body Syst.* **51**, 249 (2011).
- [13] E. Braaten and H-W. Hammer, *Phys. Rev. A* **67**, 042706 (2003).
- [14] R. Brühl *et al.*, *Phys. Rev. Lett.* **95**, 06002 (2005).
- [15] T. Kraemer *et al.*, *Nature* **440**, 315 (2006).
- [16] S. Knoop *et al.*, *Nat. Phys.* **5**, 227 (2009).
- [17] M. Zaccanti, *et al.*, *Nat. Phys.* **5**, 586 (2009).
- [18] N. Gross *et al.*, Z. Shotan, S. Kokkelmans, and L. Khaykovich, *Phys. Rev. Lett.* **103**, 163202 (2009).
- [19] S. E. Pollack, D. Dries and R. G. Hulet, *Science* **326**, 1683 (2009).
- [20] T.B. Ottenstein, T. Lompe, M. Kohnen, A.N. Wenz, S. Jochim, *Phys. Rev. Lett.* **101**, 203202 (2008).
- [21] J.R. Williams *et al.*, *Phys. Rev. Lett.* **103**, 130404 (2009).
- [22] T. Lompe *et al.*, *Science* **330**, 940 (2010).
- [23] S. Nakajima, M. Horikoshi, T. Mukaiyama, P. Naidon, and M. Ueda, *Phys. Rev. Lett.* **105**, 023201 (2010).
- [24] S. Nakajima, M. Horikoshi, T. Mukaiyama, P. Naidon, and M. Ueda, *Phys. Rev. Lett.* **106**, 143201 (2011).
- [25] R. Lazauskas and J. Carbonell, *Phys. Rev. A* **73**, 062717 (2006).
- [26] P. Barletta and A. Kievsky, *Phys. Rev. A* **64**, 042514 (2001).
- [27] V.A. Roudnev, S.L. Yakovlev and S.A. Sofianos, *Few-Body Syst.* **37**, 179 (2005).
- [28] M. Lewerenz, *J. Chem. Phys.* **106**, 4596 (1977).
- [29] D. Bressanini, M. Zavaglia, M. Mella and G. Morosi, *J. Chem. Phys.* **112**, 717 (2000).
- [30] D. Blume and C.H. Greene, *J. Chem. Phys.* **112**, 8053 (2000).
- [31] T.K. Das, B. Chakrabarti and S. Canuto, *J. Chem. Phys.* **134**, 164106 (2011).
- [32] V.R. Pandharipande *et al.*, J.G. Zabolitzky, S.C. Pieper, R.B. Wiringa and U. Helmbrecht, *Phys. Rev. Lett.* **50**, 1676 (1983).
- [33] Th. Cornelius and W. Gloeckle, *J. Chem. Phys.* **85**, 3906 (1986).
- [34] J. Carbonell, C. Gignoux and S.P. Merukriev, *Few-Body Syst.* **15**, 15 (1993).
- [35] E. Nielsen, D.V. Fedorov and A.S. Jensen, *J. Phys. B* **31**, 4085 (1998).
- [36] V. Roudnev and S. Yakovlev, *Chem. Phys. Lett.* **328**, 97 (2000).
- [37] A.K. Motovilov, W. Sandhas, S.A. Sofianos and E.A. Kolganova, *Eur. Phys. J. D* **13**, 33 (2001).
- [38] E.A. Kolganova, A.K. Motovilov and W. Sandhas, *Phys. Rev. A* **70**, 052711 (2004).
- [39] H. Suno and B.D. Esry, *Phys. Rev. A* **78**, 062701 (2008).
- [40] M. Kamimura, *Phys. Rev. A* **38**, 621 (1988).

- [41] H. Kameyama, M. Kamimura and Y. Fukushima, Phys. Rev. C **40**, 974 (1989).
- [42] M. Kamimura and H. Kameyama, Nucl. Phys. **A508**, 17c (1990).
- [43] E. Hiyama, Y. Kino and M. Kamimura, Prog. Part. Nucl. Phys. **51**, 223 (2003).
- [44] E. Hiyama and T. Yamada, Prog. Part. Nucl. Phys. **63**, 339 (2009).
- [45] E. Hiyama *et al.*, Prog. Theor. Phys. Supplement **185**, 1 (2010); **185**, 106 (2010); **185**, 152 (2010).
E. Hiyama, Few-Body Systems, to be published (2012).
- [46] J.L. Friar, B.F. Gibson, D.R. Lehman and G.L. Payne, Phys. Rev. C **25**, 1616 (1982).
- [47] H.M. Xu, C.A. Gagliardi, R.E. Tribble, A.M. Mukhamedzhanov and N.K. Timofeyuk, Phys. Rev. Lett. **73**, 2027 (1994).
- [48] A.M. Mukhamedzhanov *et al.*, Phys. Rev. C **56**, 1302 (1997).
- [49] E. Hiyama, M. Kamimura, A. Hosaka, H. Toki and M. Yahiro, Phys. Lett. B **633**, 237 (2006).
- [50] E. Hiyama, M. Kamimura, Y. Yamamoto, and T. Motoba, Phys. Rev. Lett. **104**, 212502 (2010).
- [51] P. Naidon, E. Hiyama and M. Ueda, arXiv:1109.5807v1 [physics.atom-ph].
- [52] V. Roudnev and M. Cavagnero, J. Phys. B: At. Mol. Opt. Phys. **45**, 025101 (2012).
- [53] G.L. Payne and B.F. Gibson, Few-Body Systems **14**, 117 (1993).
- [54] K. Ogata, S. Hashimoto, Y. Iseri, M. Kamimura and M. Yahiro, Phys. Rev. C **73**, 024605 (2006).
- [55] H. Kamada, A. Nogga, W. Glockle, E. Hiyama, M. Kamimura, K. Varga, Y. Suzuki, M. Viviani, A. Kievsky, S. Rosati, J. Carlson, Steven C. Pieper, R. B. Wiringa, P. Navratil, B. R. Barrett, N. Barnea, W. Leidemann, and G. Orlandini, Phys. Rev. C **64**, 044001 (2001).
- [56] E. Hiyama, B.F. Gibson and M. Kamimura, Phys. Rev. C **70**, 031001(R) (2004).
- [57] C. Kurokawa and K. Kato, Phys. Rev. C **71**, 021301 (2005).
- [58] Y. Funaki *et al.*, Phys. Rev. Lett. **101**, 082502 (2008).